Zeolite catalysts for Halon conversion

Russell F. Howe [a,b,*], Stuart Thomson [b], Yannan Yang [b], Kai Lee [c],
Eric M. Kennedy [c], Bogdan Z. Dlugogorski [c]

[a] *Chemistry Department, University of Aberdeen, Aberdeen AB24 3UE, Scotland, UK*
[b] *Chemistry Department, University of New South Wales, New South Wales, Australia*
[c] *Department of Chemical Engineering, University of Newcastle, Newcastle, Australia*

Abstract

Al and Ni K-edge XANES and EXAFS experiments have been undertaken to characterise the chemical states of aluminium and nickel in NiZSM-5 catalysts used for the pyrolysis and hydrodehalogenation with methane of Halon 1301 (CF_3Br). It is shown that pyrolysis of Halon 1301 over NiZSM-5 involves both extra-framework aluminium fluoride or hydroxyfluoride species and aggregated nickel species, probably fluorided. Reaction products are CF_4 and C_2F_6. The reaction between Halon 1301 and methane over NiZSM-5 produces CHF_3 and CH_3Br as major, but not exclusive products. In the presence of CH_4 framework dealumination and aggregation of nickel is inhibited. Future prospects for utilising these and similar catalysts in reactions of other Halons and CFCs to produce useful fluorocarbon products as an alternative to destruction are briefly discussed. © 2002 Elsevier Science B.V. All rights reserved.

Keywords: Zeolites; Halons; XANES; EXAFS; NiZSM-5; Methane

1. Introduction

The well known problem of stratospheric ozone depletion by chlorine and bromine containing compounds has been addressed through the Montreal protocol, which in its more recent revisions calls for a phase out in the production of Halons (bromine containing fluorocarbons and chlorofluorocarbons) by 1994, and of CFCs by 1996. The use of CFCs in developed countries is now banned, and many countries are moving to ban the use of Halons. This legislation has initiated extensive research into possible replacements for Halons and CFCs, and to a lesser extent into methods for disposal of existing stockpiles.

A number of destruction technologies for CFCS and Halons are currently in use or under development. Thermal incineration, an established method, is energy inefficient and produces environmentally hazardous by-products; the alternative plasma arc process is environmentally more acceptable, but much more expensive [1]. Other lower temperature catalytic destruction processes are being studied, but catalyst deactivation remains a problem [2,3].

Given the high initial costs of producing Halons and CFCs, there is a considerable incentive to find non-destructive processes which remove the ozone depleting bromine and chlorine atoms while retaining the carbon–fluorine bonds, forming fluorocarbons (FCs) or hydroflurocarbons (HFCs). These materials are not ozone depleting, and have value as products.
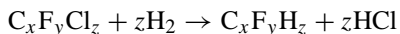
A number of groups are investigating catalytic hydrodechlorination of CFCs as a route to HFCs [4–12].

The general chemistry required can be represented as follows:

$$C_xF_yCl_z + zH_2 \rightarrow C_xF_yH_z + zHCl$$

Supported palladium catalysts appear to be the most active, and show the highest selectivities for retention of C–F bonds (the undesired reaction pathway is the complete hydrogenation of the CFC to an alkane, forming HF as well as HCl). It is noteworthy that fluorided supports show particularly high activity and selectivity. Coq et al. [4,5] showed that oxide supports were converted to fluoride supports during the reaction of CCl_2F_2 with hydrogen over supported palladium. The reaction of oxides such as alumina or zirconia with fluorocarbons is known to cause replacement of oxide and hydroxide ions with fluoride ions [6]. Other workers have claimed that a surface palladium carbide phase is the active component in supported palladium catalysts [7]. Promotion of palladium–silica catalysts with bismuth or thallium was found by Ohnishi et al. to dramatically enhance the selectivity to olefinic products in the hydrodehalogenation of CCl_2FCClF_2 [8]. Karpinski et al. studied the hydrodehalogenation of the closely related CFC CCl_2CF_3, over palladium–alumina and found that a high hydrogen over-pressure was needed to maintain selectivity to the desired HCF product CH_2FCF_3 [9].

Metals other than palladium are less active for hydrodehalogenation, but may show different product selectivities. For example, reaction of CF_2Cl_2 with hydrogen over ruthenium supported on carbon or magnesium fluoride gave high selectivities to the mono-substituted product CF_2HCl [10]. Similar selectivity to the mono-substituted product $CHClFCF_3$ was observed for the reaction of CCl_2FCF_3 with hydrogen over silica supported ruthenium [11], while CCl_3CF_3 over the same catalysts forms C_4 coupling products [12].

Despite this attention paid to CFCs, there appear to be no reports in the open literature of catalytic hydrodehalogenation of Halons. Halons 1211 (CF_2ClBr), 1301 (CF_3Br) and 2402 ($C_2F_4Br_2$) are all used as fire retarding agents, and have ozone depleting potentials considerably higher than CFCs. The homogeneous gas phase reaction of CF_2ClBr with hydrogen is reported to begin above 673 K, forming CHF_2Cl, CHF_2Br, CH_2F_2 and CH_4 [13], while the reaction of CF_3Br with hydrogen can be enhanced by

UV irradiation, forming CHF_3 [14]. Thermal reaction of CF_3Br with hydrogen has been studied more recently by three of the present authors; conversions of 80% were achieved at 973 K and 1 s residence time, with a selectivity to CHF_3 in excess of 80% [15].

Li et al. [16,17] studied the homogeneous gas phase pyrolysis of CF_3Br over the temperature range 673–1073 K, with residence times between 0.1 and 2.0 s. The homogeneous reaction begins at about 873 K, and the conversion increases exponentially with increasing temperature. The major carbon containing products are C_2F_6 and CF_4; at low temperatures the selectivity to C_2F_6 is close to 100%, but CF_4 yield increases with increasing temperature. C_2F_6 formation can be envisaged to involve dimerisation of two CF_3 radicals:

$$2CF_3Br \rightarrow C_2F_6 + Br_2$$
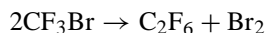
Bromine was detected as a reaction product, although not quantified. CF_4 formation, on the other hand, must involve C–F bond cleavage.

The authors were able to model the observed conversions and selectivities with a 12 step reaction mechanism [17]. The initial reaction step is thermal cleavage of the C–Br bond:
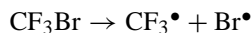
$$CF_3Br \rightarrow CF_3^\bullet + Br^\bullet$$

followed by attack of a bromine atom on a second CF_3Br molecule:
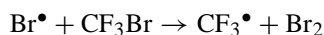
$$Br^\bullet + CF_3Br \rightarrow CF_3^\bullet + Br_2$$

C_2F_6 is generated by recombination of two CF_3 radicals. CF_4 may be formed from attack of $CF_3^\bullet$ on a further CF_3Br molecule:

$$CF_3^\bullet + CF_3Br \rightarrow CF_4 + CF_2Br^\bullet$$
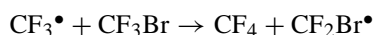
Further subsequent reactions lead to the formation of minor products such as CBr_2F_2 and termination of the chain reaction.

We were interested to determine if the reaction rates and product selectivities for this pyrolysis reaction could be altered by intercepting the reaction pathway with zeolite catalysts. Konya et al. have described the adsorption and decomposition of CFCs over different Y zeolites [18]. They observed a dominant role of zeolite acidity in the decomposition, and found by infrared spectroscopy that transition metal ions

enhanced both the formation and decomposition of phosgene as a surface intermediate in the decomposition process. Phosgene could also be detected in the gas phase at elevated temperatures. The authors inferred that phosgene formation involved continuous dealumination of the zeolite framework, i.e. the decomposition reaction was stoichiometric rather than catalytic.

Zeolite ZSM-5 is known to have a structure which tolerates very substantial framework dealumination, and can have strong Bronsted acidity. Accordingly, we examined the pyrolysis of CF_3Br in the presence of HZSM-5 and a Ni^{2+} exchanged ZSM-5 [16]. NiZSM-5 in particular significantly enhances the decomposition reaction, and catalytic decomposition begins at temperatures 200 K lower than the homogeneous gas phase reaction. There is initially 100% conversion of CF_3Br over NiZSM-5 at this temperature for the first 50 min on stream, followed by deactivation to a steady state conversion of around 25%. During the initial period of high activity, the major carbon containing product detected is CF_4, with 70% selectivity, but during the later deactivation this falls to around 10% and C_2F_6 becomes the major product. For HZSM-5, on the other hand, the initial high conversion of CF_3Br is immediately lost, and the steady state conversion falls to less than 10%, only slightly higher than the homogeneous gas phase value at this temperature. C_2F_6 is the only significant carbon containing product detected over HZSM-5.

We have also reported previously the hydrodehalogenation of CF_3Br over transition metal exchanged ZSM-5 zeolites, using methane rather than hydrogen as the source of hydrogen atoms [19,20]. Methane is available at low cost from natural gas, offers multiple hydrogen atoms per molecule, and in principle forms alkyl halide products rather than corrosive hydrogen halides. A homogeneous gas phase reaction occurs between CF_3Br and CH_4 on heating above 850 K. The kinetics and product distributions obtained in this reaction have been described in [17]. At temperatures below 900 K there is an approximately equal conversion of the two reactants, and the major products are those expected for simple halogen exchange:

$$CH_4 + CF_3Br \rightarrow CH_3Br + CHF_3$$
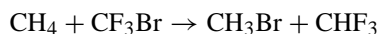
As in the pyrolysis reaction described above, the reaction is considered to be initiated by thermal cleavage of C–Br bonds generating CF_3 radicals. These then attack CH_4, forming CHF_3 and CH_3 radicals; the CH_3 radicals then strip a bromine atom from a further CF_3Br molecule. At higher temperatures, the conversion of methane falls below that of CF_3Br, and other products such as $C_2H_2F_2$, C_2H_4 and $CHBrF_2$ appear in minor yields. The variations of product selectivities with temperature and reactant feed ratio could be adequately simulated with a multi-step free radical mechanism.

Interception of this reaction with zeolite catalysts lowers substantially the temperature required for significant conversion. At 873 K, the initial conversions of CF_3Br and CH_4 over HZSM-5 are 10-fold higher than those of the homogeneous reaction at the same flow rate, but the catalyst deactivates over a 2 h period to steady state conversions which are only slightly higher than those in the homogeneous reaction. On the other hand, the NiZSM-5 catalyst, after an initial break in period, maintains high steady state conversions for more than 20 h before beginning to slowly deactivate. The steady state conversion of CF_3Br over NiZSM-5 exceeds that of methane under all conditions. The product selectivities over the NiZSM-5 catalyst were found to vary little with time on stream. Steady state selectivities at 873 K were around 40% to CH_3Br, 30% to CHF_3, 12% to CH_2Br_2, and around 5–6% to minor products C_2F_6, C_2H_4, C_2H_2 and $C_2H_2F_2$. The activity of used nickel catalysts could be regenerated almost completely by treatment in a hydrogen stream at 623 K for 3 h, whereas an oxidative treatment (expected to remove coke) had little effect [20]. Catalytic performance similar to that achieved with NiZSM-5 is also seen with CuZSM-5 and MnZSM-5 [19].

In order to better understand the changes occurring in the zeolite catalysts during pyrolysis and hydrodehalogenation of CF_3Br, we have carried out detailed characterisation studies on fresh catalysts and on samples removed from the reactor at various times on stream. This paper describes in particular new results obtained using Al and Ni K-edge XANES and EXAFS to monitor changes in the coordination and chemical environment occurring during catalyst break-in and deactivation.

2. Experimental

Experimental details of catalysts used in our work, of the plug flow microreactor used for catalyst testing and of the standard characterisation techniques employed can be found in previously published articles [16,20]. Al K-edge XANES data were measured in total electron yield mode (channeltron detector) on Beam Line 3-3 at the Stanford Synchrotron Radiation Laboratory. Pressed discs of catalyst were mounted using conducting tape on a sample holder inserted into a vacuum chamber (10^{-6} Torr) interfaced to the beam line via a diamond window. A $YB_{66}(400)$ double crystal monochromator was used, and spectra collected in step-scan mode at room temperature. Ni K-edge EXAFS data were measured in transmission mode at Beam Line 20B (the Australian National Beam Line Facility) at the Photon Factory, Japan, using a Si(1 1 1) monochromator. Processing and fitting of the EXAFS data was undertaken with the program XFIT [21].

3. Results and discussion

3.1. Pyrolysis of CF_3Br

Remarkably, X-ray diffraction patterns of used catalysts showed no loss of zeolite crystallinity, even after many hours on stream at reaction temperatures, and chemical analysis showed no loss of aluminium or nickel. ^{27}Al NMR spectra showed however that the characteristic signal of tetrahedral framework aluminium in the fresh zeolite catalysts was completely lost after exposure to CF_3Br for only a few minutes at 973 K. This loss of framework aluminium was confirmed in ^{29}Si spectra, which showed a narrowing of line width typical of a dealuminated framework. NiZSM-5 catalysts exposed to CF_3Br on stream for several hours or more gave a new signal in the ^{27}Al NMR spectrum characteristic of octahedral aluminium. The appearance of this signal coincided with the deactivation of the catalyst and the change in product selectivity referred to above. These changes in the NMR spectra were interpreted in terms of a two stage process (at least for NiZSM-5), in which exposure to CF_3Br causes rapid removal of aluminium from the zeolite framework to form a low symmetry

extra-framework aluminium species which is NMR invisible, followed by conversion of this species to an octahedral extra-framework species.

XPS analysis of the used catalyst samples revealed that there was a significant depletion of surface aluminium from the zeolites; in the case of HZSM-5 aluminium could no longer be detected by XPS after 9 h on stream. XPS also showed however that high concentrations of surface fluorine are present in used catalysts. For example, after 9 h on stream, a NiZSM-5 catalyst gave an F:Si ratio of 0.167 by XPS, which was reduced appreciably on argon ion sputtering [16].

Oxides such as alumina are known to undergo halogen exchange reactions with halocarbons. This chemistry has been extensively studied by Kemnitz and Menz, and recently reviewed [6]. A sample of γ-alumina was accordingly tested for CF_3Br pyrolysis activity. It was found that although high conversions of CF_3Br were measured for short periods of time at temperatures as low as 773 K, negligible amounts of fluorocarbon products were detected, and examination of the used catalyst by X-ray powder diffraction showed that it had been quantitatively converted to β-AlF_3. This clearly results from a stoichiometric reaction between γ-alumina and CF_3Br. Although we have not studied in detail the chemistry of this reaction, the resulting bulk phase appears to have little catalytic activity for the pyrolysis reaction.

The reaction with γ-alumina provides some clues about what may be occurring with the zeolite catalyst. The substitution of fluorine into alumina through reaction with $CHClF_2$ occurs via hydroxyfluoride intermediate phases [22], and similar chemistry occurring with CF_3Br at Bronsted acid sites in the zeolite catalysts would be expected to form aluminium hydroxyfluoride species which may be partially or completely detached from the zeolite framework, e.g.
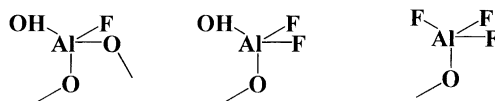
Such species would contain aluminium in a low symmetry environment, and the resulting quadrupolar broadening would render them invisible to the conventional one pulse NMR experiment. A spectroscopic signature of aluminium fluoride species can be obtained however from the aluminium K-edge XANES
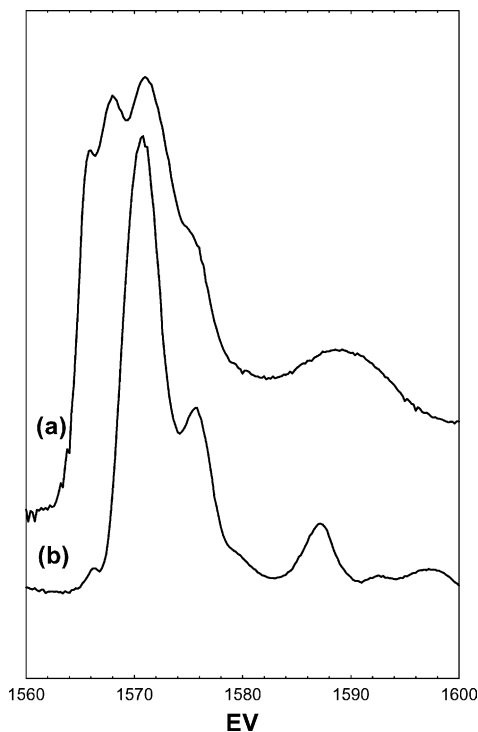
Fig. 1. Aluminium K-edge XANES spectra of (a) γ-Al$_2$O$_3$ and (b) β-AlF$_3$ formed by reaction with CF$_3$Br up to 973 K.

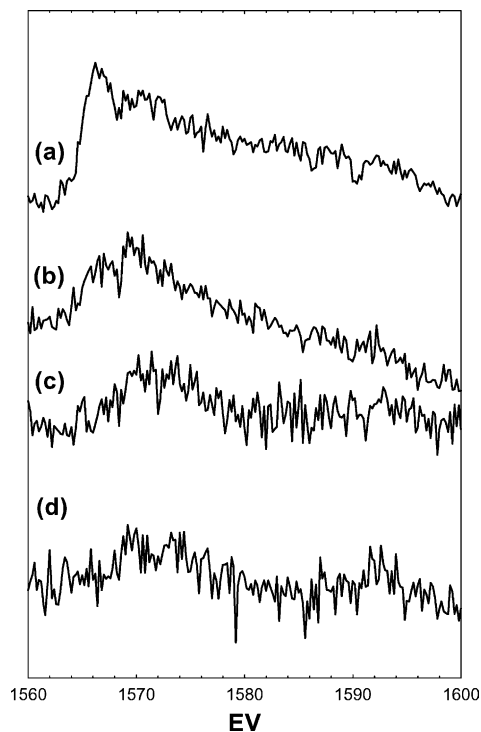Fig. 2. Aluminium K-edge XANES spectra of (a) fresh NiZSM-5 catalyst, and following exposure to CF$_3$Br at 973 K for (b) 20 min; (c) 90 min; and (d) 6 h.

spectrum. The K-edge XANES spectrum arises from X-ray excited electronic transitions from the 1 s orbital to higher bound states. The energies of these states and therefore the observed X-ray absorption energies are sensitive to the coordination environment.

Fig. 1 shows Al XANES spectra of γ-alumina before and after exposure to CF$_3$Br at 773 K for 4 h and 973 K for 2 h. The X-ray diffraction pattern of the treated sample confirmed it to be β-AlF$_3$. The XANES of the AlF$_3$ phase is closely similar to that reported previously by Grohman et al. [23], comprising a strong white line peak (the dipole allowed 1 s to 2p transition) at 1570 eV with a higher energy shoulder. It is noteworthy that the white line peak is shifted to higher energy by about 4 eV relative to the first peak in the alumina spectrum.

Fig. 2 shows a series of Al K-edge XANES spectra measured from NiZSM-5 catalysts before and after reaction with CF$_3$Br at 973 K for various lengths of time. The aluminium content of the zeolite is low

(Si:Al = 50), which means that the signals observed are very weak. The fresh catalyst shows a XANES spectrum characteristic of aluminium in tetrahedral coordination in a zeolite framework [24]. After brief exposure to CF$_3$Br at 973 K, the white line signal of tetrahedral framework aluminium is replaced by a new signal at higher energy which is in the identical position to that measured from the alumina sample converted to β-AlF$_3$. This new signal is reduced in intensity in catalyst samples removed from the reactor after longer times on stream, and can be barely detected after 6 h of reaction. The loss of intensity is consistent with XPS results showing depletion of surface aluminium, since both techniques measure surface composition only. The Al XANES data do indicate however that the aluminium remaining in the surface layers of the zeolite is in a fluoride environment.

As described by Li et al. [16], FTIR measurements of pyridine chemisorption show that used catalysts contain both Bronsted and Lewis acidity. In the case

of HZSM-5, the acid sites can no longer be detected after the catalyst has been on stream for several hours, whereas in NiZSM-5 acid sites are still present after 9 h on stream. Bronsted and Lewis acidity are both found in alumina catalysts partially halogen exchanged with $CHClF_2$ [22]. The fluoride and hydroxyfluoride extra-framework aluminium species that we propose are formed on exposure of the zeolite catalysts to CF_3Br would be expected to show similar acidic properties.

The coordination state of the Ni ions in NiZSM-5 is also changed on exposure to CF_3Br at reaction temperatures. This can be clearly seen in the Ni K-edge EXAFS Fourier transforms presented in Fig. 3. The fresh catalyst contains Ni in ion exchange sites, showing a single oxygen coordination shell. After brief exposure to CF_3Br at 973 K, the intensity of the first shell is reduced and a strong second shell appears due to Ni–Ni interactions at a distance (after phase correction) of 0.296 nm. As shown in Fig. 4 the observed
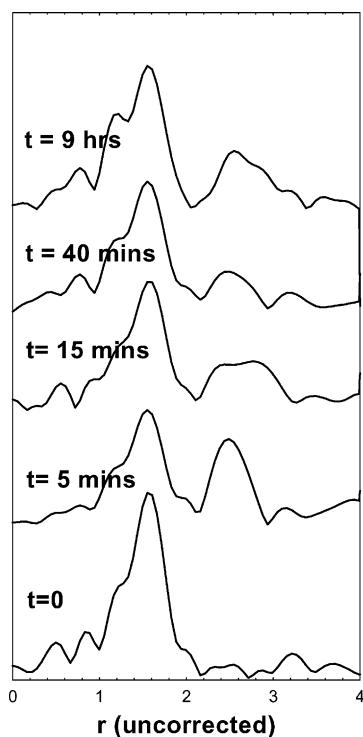

Fig. 3. Nickel K-edge EXAFS Fourier transforms of a fresh NiZSM-5 catalyst, and following exposure to CF_3Br at 973 K for different times.

Fourier transform of the catalyst taken from the reactor after 5 min exposure to CF_3Br can be fitted equally well to two different structural models: NiO, with 4.5 oxygens at a distance of 0.203 nm and 3.2 nickels at a distance of 0.296 nm, or NiF_2, with 3.8 fluorines at a distance of 0.201 nm and the same Ni:Ni parameters as the first model. EXAFS is unable to clearly differentiate between oxygen and fluorine nearest neighbors, given the similarity of the back scattering amplitude and phase shift parameters for these two atoms. The observed Ni–Ni distance is close to those in both NiO (0.297 nm) and NiF_2 (0.308 nm) [25]. The first shell Ni–F distance is close to the longer of the Ni–F distances in NiF_2 (0.2018 nm), whereas the fitted Ni–O distance is significantly shorter than that in NiO (0.2097 nm). However, we cannot conclude unambiguously from these data that a nickel fluoride species is formed, even if the alternative nickel oxide species seems chemically less plausible. What is clear is that whatever the nickel species is that is formed in the zeolite pores on initial exposure to CF_3Br remains unchanged throughout the lifetime of the catalyst. This species comprises NiF_2 or NiO clusters dispersed within the zeolite pores (since there is no surface enrichment of Ni detected by XPS). The Fourier transforms in Fig. 3 show a broadening of the second shell Ni:Ni peak at longer reaction times, indicating increasing disorder in the system, but there is no other obvious change in the state of the nickel.

To summarise, from the characterisation experiments on used catalyst samples, the following conclusions can be drawn about the chemistry occurring during pyrolysis of CF_3Br.

- There is rapid attack of CF_3Br on Bronsted acid sites in the zeolites, producing extra-framework aluminium fluoride and/or hydroxyfluoride species.
- The acid sites associated with the extra-framework aluminium species promote the formation of C_2F_6, but these sites are rapidly deactivated in HZSM-5.
- In NiZSM-5 an extra-framework nickel species is rapidly formed which may be a fluoride species; this appears to promote CF_4 formation.
- CF_4 formation at Ni sites is inhibited after about 2 h on stream at 973 K, but C_2F_6 formation at acid sites continues, i.e. the deactivation of sites responsible for C_2F_6 formation in HZSM-5 does not occur in the NiZSM-5 zeolite.
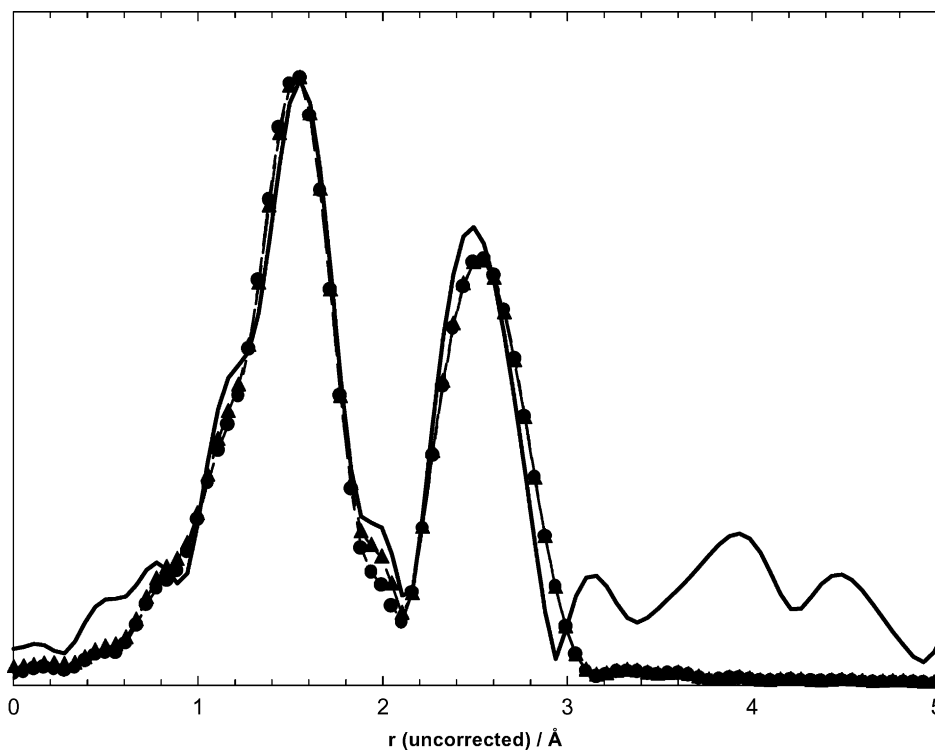
Fig. 4. Comparison of observed and fitted nickel K-edge EXAFS Fourier transforms for a NiZSM-5 catalyst exposed to CF_3Br at 973 K for 5 min. Solid line: observed data; dashed line (circles): fitted data for a first shell of 4.5 oxygens at a distance of 0.203 nm and 3.2 nickels at 0.296 nm; dashed line (triangles): fitted data for a first shell of 3.8 fluorines at 0.201 nm and 3.2 nickels at 0.296 nm.

• The ZSM-5 zeolite framework survives exposure to CF_3Br at elevated temperatures.

3.2. Reaction of CF_3Br with methane

As for the pyrolysis reaction, X-ray diffraction measurements on the zeolite catalysts used for the hydrodehalogenation reaction show that the zeolite structures remain intact, and ^{27}Al NMR measurements show that tetrahedral framework aluminium is lost, although not as rapidly as in the case of pyrolysis. Fig. 5 shows aluminium K-edge XANES spectra of a fresh NiZSM-5 zeolite and of catalyst samples taken from the reactor after 15 min and 3 h on stream. This again indicates the formation of aluminium fluoride species, as revealed by the ca. 4 eV shift in position of the white line peak to higher energy (in comparison with Fig. 1). The signal intensity remains however significantly higher than for the same catalysts used

in pyrolysis of CF_3Br, suggesting there is less loss of surface aluminium.

An explanation for these differences can be offered in terms of the established gas phase mechanism for the reaction. If it is assumed that attack of CF_3 radicals on Bronsted acid sites causes framework dealumination and formation of extra-framework aluminium fluoride or hydroxyfluoride species, methane will intercept these radicals and inhibit to some extent the dealumination process. It is noteworthy that the lifetime of the HZSM-5 zeolite is considerably longer for the reaction of CF_3Br with methane than it is for the pyrolysis reaction.

There is also a significant difference in the behaviour of the nickel in NiZSM-5 between the reaction with methane and the pyrolysis reaction. Fig. 6 compares the Ni K-edge EXAFS Fourier transforms of the fresh NiZSM-5 catalyst and one removed from the reactor after several hours on stream. There
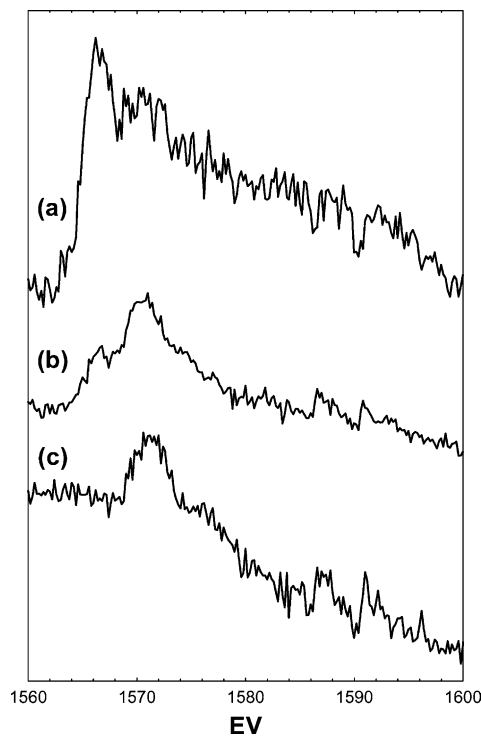
Fig. 5. Aluminium K-edge XANES spectra of (a) fresh NiZSM-5 catalyst and one used in the reaction of CF_3Br with CH_4 at 873 K for (b) 15 min; and (c) 3 h.

Fig. 6. Nickel K-edge EXAFS Fourier transforms of a fresh NiZSM-5 catalyst and one used in the reaction of CF_3Br with CH_4 at 873 K for 3 h.

is no indication of any strong Ni:Ni interactions appearing in the Fourier transform of the used catalyst. As noted above, EXAFS is unable to determine if the original oxygen coordination shell has been replaced by fluorine in the used catalyst, but it is certain that the formation of extra-framework NiF_2 or NiO clusters seen in used pyrolysis catalysts is not occurring in the presence of methane. The ability of a hydrogen treatment to restore the activity of a used catalyst is similar to that reported for Rh–SiO_2 catalysts deactivated by chlorine during the hydrodechlorination of trichloroethylene [26]. This suggests that fluorine deposition in the NiZSM-5 may be responsible for the deactivation occurring at longer reaction times.

The reaction chemistry of CF_3Br with methane over the NiZSM-5 catalysts is complex, but we suggest that, as in pyrolysis, cleavage of C–Br bonds is the crucial initiating step. Whether the subsequent reaction steps involve gas phase radicals (as in the homogeneous case) or adsorbed species is not yet clear.
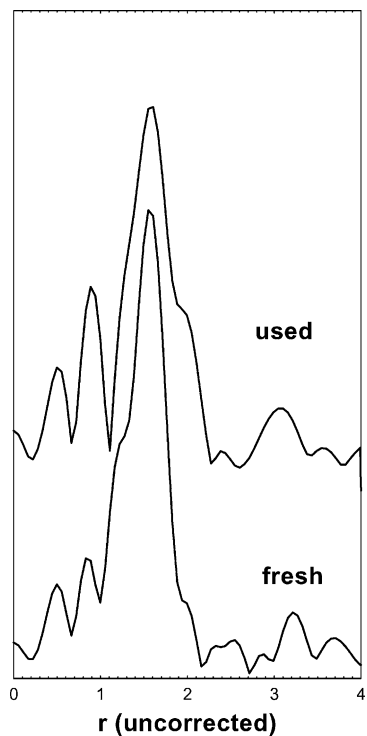
The role of the nickel cations may be to promote C–Br bond cleavage. As noted above, other transition metal exchanged ZSM-5 zeolites are also active for this reaction [19]; although we have not yet examined these catalysts in the same detail, the transition metal component is presumed to play a similar role.

3.3. Future prospects

The work to date with zeolite catalysts has established that the reaction of Halon 1301 with methane achieves the desired result of removal of bromine from the Halon. The catalytic mechanism involved is not yet clear however, and catalyst optimisation has not yet been achieved. In particular, further improvement of the selectivity to CHF_3 is desirable. Although ZSM-5 zeolites offer the advantages of high surface area, stable framework structure and facile dealumination to form the extra-framework aluminium species which appear to be important in this chemistry, other

zeolites such as beta may provide similar advantages. Other high surface area supports for the transition metal component also need to be explored.

The product of hydrodebromination of Halon 1301, CHF_3, has potential as a precursor for the production of the replacement for the Halon, CF_3I. This material, known commercially as triiodide, is non-ozone depleting and has fire suppressant properties only slightly inferior to those of Halons [27]. A new catalytic technology for CF_3I production from CHF_3 has been recently described [28]. This involves gas phase reaction of CHF_3 with I_2 in the presence of oxygen over a carbon supported alkali metal salt catalyst, at temperatures between 400 and 600 °C. The reaction ostensibly could be written as

$$CHF_3 + I_2 \rightarrow CF_3I + HI$$
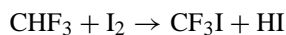
but it has been shown that the actual reaction stoichiometry is [29]

$$3CHF_3 + I_2 \rightarrow 2CF_3I + C + 3HF$$

The role of oxygen in the reaction is to inhibit carbon deposition and poisoning of the catalyst.

The pyrolysis and/or hydrodehalogenation of other Halons offers further opportunities for catalysis. For example, the elimination of bromine from Halon 2402 may provide a useful route to perfluoroethene:

$$C_2F_4Br_2 \rightarrow C_2F_4 + Br_2$$
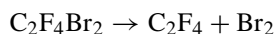
The homogeneous reaction of Halon 1211 with methane in the gas phase has been shown recently to give high yields of the coupling product $C_2H_2F_2$ at 1073 K [30]. This reaction can be formally written as

$$CF_2ClBr + CH_4 \rightarrow CF_2CH_2 + HCl + HBr$$

although the actual reaction pathway is more complex than this, involving free radical abstraction and coupling reactions. The possibility of enhancing this reaction at lower temperatures with heterogeneous catalysts is intriguing, both from the viewpoint of Halon conversion to useful products, and from the more fundamental aspect of catalytic methane activation.

Finally, the catalytic hydrodehalogenation of CFCs with methane rather than hydrogen clearly needs to be pursued further, given the success of this process with Halons. The catalytic chemistry of fluorocarbons more generally, both synthesis and inter-conversion, offers many opportunities for innovative research, both with zeolites and with other types of catalyst.

Acknowledgements

References

[1] G.M. Bickle, T. Suzuki, Y. Mitarai, Chem. Eng. Trans. I 70 (1992) 449.

[2] M. Tajima, M. Niwa, Y. Fujii, Y. Koinuma, R. Aizawa, S. Kushiyama, S. Kobayashi, K. Mizuno, H. Ohuchi, Appl. Catal. B14 (1997) 97.

[3] K.U. Niedersen, E. Lieske, E. Kemnitz, Green Chem. 1 (1999) 225.

[4] B. Coq, J.M. Cognion, F. Figueras, D. Tournigant, J. Catal. 141 (1993) 21.

[5] B. Coq, F. Figueras, S. Hub, D. Tournigant, J. Phys. Chem. 99 (1995) 11159.

[6] E. Kemnitz, D.H. Menz, Progr. Solid State Chem. 26 (1998) 97.

[7] W. Juszczyk, A. Malinowski, Z. Karpinski, Appl. Catal. A166 (1998) 311.

[8] R. Ohnishi, W.L. Wang, M. Ichikawa, Appl. Catal. A113 (1994) 29.

[9] Z. Karpinski, K. Early, J. D'Itri, J. Catal. 164 (1996) 378.

[10] A. Malinowski, W. Juszczyk, M. Bonarowska, M. Wojciechowska, Z. Kowalczyk, Z. Karpinski, React. Kinet. Catal. Lett. 68 (1999) 53.

[11] T. Mori, Y. Morikawa, Elsevier studies in surface science and catalysis 130 (2000) 1985.

[12] T. Mori, W. Ueda, Y. Morikawa, Catal. Lett. 38 (1996) 73.

[13] H.J.P. de Lijser, R. Louw, P. Mulder, J. Chem. Soc., Perkin Trans. II (1994) 139.

[14] S. Gulati, M. Lavid, Chemical Processes in Combustion, 1993, p. 69.

[15] K. Li, E.M. Kennedy, B. Moghtaderi, B.Z. Dlugogorski, et al., Environ. Sci. Tech. 34 (2000) 584.

[16] K. Li, F. Oghanna, E.M. Kennedy, B.Z. Dlugogorski, A. Fazeli, S. Thomson, R.F. Howe, Microp. Mesop. Mater. 35/36 (2000) 219.

[17] K. Li, E.M. Kennedy, B.Z. Dlugogorski, Chem. Eng. Sci. 55 (2000) 4067.

[18] Z. Konya, I. Kannus, I. Kiricsi, Elsevier studies in surface science and catalysis 105 (1997) 1509.

[19] K. Li, E.M. Kennedy, B. Dlugogorski, R.F. Howe, Chem. Commun. (1999) 709.

[20] K. Li, E.M. Kennedy, B. Dlugogorski, R.F. Howe, Catal. Today 63 (2000) 355.

[21] P.A. Ellis, H.C. Freeman, J. Synchrotron Rad. 2 (1995) 190.

[22] A. Hess, E. Kemnitz, A. Lippitz, W.E.S. Unger, D.H. Menz, J. Catal. 148 (1994) 270.

[23] I. Grohman, A. Hess, E. Kemnitz, W. Feintrup, W.E.S. Unger, J. Wong, M. Rowen, T. Tanaka, M. Froba, J. Mater. Chem. 8 (1998) 1453.

[24] J.A. van Bokhaven, H. Sambe, D.E. Ramaker, D.C. Koningsberger, J. Phys. Chem. 103B (1999) 7537.

[25] Gmelin Handbuch der Anorganische Chemie, Springer, Berlin, 1980.

[26] J.W. Bozelli, Y.M. Chen, Chem. Eng. Commun. 115 (1992) 1.

[27] R.E. Tapscott, S.R. Skaggs, D. Dierdorf, Am. Chem. Soc. Symp. Ser. 611 (1995) 151.

[28] N. Nagasaki, N. Suzuki, S. Nakano, N. Kunihiro, US Patent 5,892,136 (1999).

[29] N. Nagasaki, N. Suzuki, S. Nakano, N. Kunihiro, in: Proceedings of the CF_3I Symposium, Newcastle, Australia, 2000.

[30] R. Tran, E.M. Kennedy, B.Z. Dlugogorski, Ind. Eng. Chem. Res. 40 (2001) 3139.